Journal of Organometallic Chemistry 769 (2014) 58–63

Contents lists available at ScienceDirect

Journal of Organometallic Chemistry

journal homepage: www.elsevier.com/locate/jorganchem

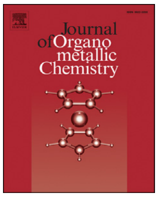

Iron selenide nanoparticles coated on carbon nanotubes from single source ferrocene incorporated selenourea precursor for fuel cell and photocatalytic applications

Raja Azadar Hussain [a], Amin Badshah [a, *], Shafiqullah Marwat [a], Farida Yasmin [a], Muhammad Nawaz Tahir [b]

[a] Department of Chemistry, Quaid-i-Azam University, 45320 Islamabad, Pakistan
[b] Department of Physics, University of Sargodha, Punjab, Pakistan

ARTICLE INFO

Article history:
Received 11 April 2014
Received in revised form
30 June 2014
Accepted 6 July 2014
Available online 15 July 2014

Keywords:
Ferrocene incorporated selenourea
Photocatalytic degradation
Single crystal
Fuel cell

ABSTRACT

This article presents the synthesis and characterization (multinuclear NMR, FTIR, CHNS, AAS and single crystal XRD) of a single source organometallic precursor namely 1-(4-methylbenzoyl)-3-(3-ferrocenylphenyl)selenourea for the fabrication of iron selenide (FeSe) nanoparticles (NPs) supported on multi walled carbon nanotubes (MWCNTs) which were characterized with XRD, SEM and TEM with fuel cell and photocatalytic applications.

Introduction

Utilization of fossil fuels for the production of energy is seriously under consideration for the future of world's economy and ecology. Use of batteries, fuel cells and electrochemical capacitors is being aimed over the years for environmental friendly and economical energy production. Batteries among the three are the ones which are most successfully applicable in different markets whereas capacitors are being used mainly in memory devices. Fuel cells however failed to have their penetration in the market on the basis of cost, performance and durability. So, the fuel cells which were being considered as a replacement of combustion engines once are now in competition with batteries and capacitors. Cost is the most important and practical factor which hinders the commercialization of fuel cells [1]. Number of efforts have been made to reduce the amount of precious metals in the fuel cell by using carbon supported platinum black, and platinum based bimetallic catalysts having comparatively cheap metals and Pt/X/Carbon (X = Fe, Ni, Co and other transition metals) alloyed materials [2,3]. In this article we have used FeSe nanoparticles coated on multi walled carbon nanotubes (MWCNTs) for fuel cell applications which may resolve the issue of cost for the acceptance of fuel cells in the open market.

Dying of the paper, textile, ceramics, leather, inks, food stuff and cosmetics is carried out with the compounds having azo (N=N) functionality [4]. Almost 15% of these compounds which are presently in use by the market, enter the environment and have been reported for their negative effects on the environment and biological life [5,6]. These compounds are not good in terms of their biodegradability and are presently being dealt with chemical methods (chlorination and ozonation) [7] and physical methods (flocculation, reverse osmosis and adsorption) [8]. Badr et al. have previously reported the photocatalytic degradation of methyl orange (MO) by gold silver nano-core/silica nano-shell to produce methyl(phenyl)carbamic acid [9]. Following the same concept we have carried out the degradation study of MO by FeSe nanoparticles supported on MWCNTs.

In the recent years FeSe has been synthesized with pulsed laser deposition [10,11], electrodeposition [12,13], chemical vapor deposition [14–17], chemical bath deposition [18,19], chemical vapor transport [20], spray pyrolysis [21], solid state reaction [22], molecular beam epitaxial growth [23], solid state reaction at different sintering temperatures [20], thick films from high temperature solution [24] and rapid, solvent-less reaction under autogenic pressure at elevated temperature (RAPET) [25] etc.

---

* Corresponding author. Tel.: +92 051 9064 2131.
E-mail address: aminbadshah@yahoo.com (A. Badshah).

http://dx.doi.org/10.1016/j.jorganchem.2014.07.001
0022-328X/

Different physical parameters and applications of FeSe such as photoemission spectrum [26,27], band structure, magnetic behavior, electronic structure, phonon spectrum, superconductivity, Mossbauer, Raman and XRD spectrum etc. have now been established. Conventional techniques for the fabrication of nano materials utilize precursors in different forms and batches but the use of single source precursor is advantageous because of good control on stoichiometry, flow, temperature, leak control and simple installation with safer experimentation [28]. Multiple source precursors generally utilize the reagents which are oxygen/moisture sensitive and toxic i.e. NH_3, H_2S, H_2Se, PH_3, AsH_3 and SiH_4 etc. This article deals with the synthesis and characterization (multinuclear NMR, FTIR, CHNS, AAS and single crystal XRD) of a novel FIS, its conversion to FeSe nanoparticles supported on MWCNTs and its application as electrode material in H_2-O_2 fuel cell [29] and as a photocatalyst for biodegradation of MO.

Materials and methods

Melting point was determined in a capillary tube using Gallenkamp (U.K) electrothermal melting point apparatus. Infrared spectrum was recorded on Thermoscientific NICOLET 6700 FTIR between 4000 and 400 cm^{-1}. ^1H and ^{13}C NMR spectra were recorded between 0 and 13 ppm and 0 and 210 ppm respectively on Jeol JNM-LA 500 FT-NMR. $Si(CH_3)_4$ was used as internal reference. The elemental analysis was performed using a LECO-932 CHNS analyzer while the Fe concentration was determined on an atomic absorption spectrophotometer Perkin Elmer 2380. UV-vis absorption spectra were recorded on Shimadzu 1800 spectrophotometer between 200 nm and 800 nm at absorbance of ~1. FeSe/MWCNTs were characterized with CuKα radiation of 0.154 nm between diffraction angles of 10–80. SEM images were taken on a SEM JEOL model, 5910 LV with an accelerating voltage of 20 kV at high vacuum (HV) mode and secondary electron image (SEI). The semi quantification elemental analysis to find out the weight percentage of the elements was done using OXFORD INCA energy dispersive X-Ray spectrometer 7274 (EDS). TEM images were recorded on JEOL 200 CX with a voltage value of 120 kV. Samples were prepared by dispersing them in methanol followed by sonication for 10 min and then placed on carbon coated copper grid for analysis.

Suitable single crystal of MPT was mounted on a glass fiber and the intensity data were collected on a Brucker kappa APEXII CCD diffractometer using graphite-monochromator having Mo Kα radiation ($\lambda = 0.71073$ Å) at 296 K. The structures were solved by direct methods and refined by full-matrix least squares against F^2 of data using SHELXL97 (Sheldrick, 1997) software [30]. Basic crystal data and description of diffraction experiment are given in Table 1, whereas selected bond lengths and bond angles have been presented in Table 2.

Ferrocene, metanitro aniline, sodium nitrite, diethyl ether, acetone, DMSO, Pd-charcoal, 4-methylbenzoyl chloride, and hydrazine were purchased from Sigma Aldrich. Meta ferrocenyl aniline was synthesized by a procedure reported by our group previously [18,19,21,31–36].

Experimental

Synthesis of 1-(4-methylbenzoyl)-3-(3-ferrocenylphenyl)selenourea (MPT)

MPT was synthesized in a one pot procedure by the addition of reactants in two batches inside a two neck round bottom flask under constant magnetic stirring. In first batch 0.3 g (0.00208 mol) of KSeCN was reacted with 0.27 mL (0.00208 mol) of 4-methylbenzoyl chloride to produce yellowish colored solution with a suspension of KCl in acetone. The reaction was monitored with the help of thin layer chromatography and allowed to proceed for 3 h under constant stirring. Then in the second batch, addition of 0.50 g (0.0018 mol) of meta ferrocenyl aniline was carried out and the reaction was completed after further 6 h with 71% yield (Scheme 1). Settled solid product was then washed with n-hexane and recrystallized in toluene. Decomposition temperature 138 °C. δ_H (ppm) (Acetone) 13.27 (s, 1H), 10.47 (s, 1H) 8.19–7.36 (m, 8H), 4.81 (t, *J* 1.8, 2H), 4.36 (t, *J* 1.8, 2H), 4.10 (s, 5H), 2.88 (s, 3H). δ_C (ppm) (Acetone) 180.6, 167.7, 144.5, 140.4, 139.0, 129.3, 128.7, 124.3, 122.3, 121.8, 84.3, 69.5, 69.0, 66.5, 20.9. v_{max}/cm^{-1} 3370, 3229 (b), 3131, 2950, 2928, 1644, 1608, 1521, 1495, 1450, 1375, 1258, 1153, 1071. Anal. Calc. for $C_{25}H_{22}N_2SeFeO$: C 59.88, N 5.58, H 4.39, Fe 11.17. Found: C 59.87, N 5.58, 4.36, Fe 11.15%.

Table 1
Crystal data of MPT.

	MPT
Empirical formula	C_{25} $H_{22}FeN_2OSe$
Formula weight	501.25
Temperature (K)	296
Wavelength Å	0.71073
a [Å]	9.9673 (13)
b [Å]	8.5714 (10)
c [Å]	25.616 (2)
α [°]	90
β [°]	96.138 (4)
γ [°]	90
Volume $Å^3$	2176 (4)
Crystal system	Monoclinic
Space group	P-21/c
Z	4
Density (calculated)	1.530 g/cm^3
h k l max	12, 10, 31
Absorption coefficient (μ)	2.385 mm^{-1}
F(000)	1016
Goodness-of-fit on F^2 (S)	1.01
R-Factor (%)	$R_1 = 0.04$, $wR_2 = 0.099$

Synthesis of catalyst

Cleaning and activation of MWCNTs

MWCNTs were sonicated in Branson 1510-DTH sonicator to separate the nanotubes and clean them from carbon soot. These MWCNTs were then washed with a 2 N HCl solution for 3 h under reflux to remove contaminants and activate their surface. In the next step MWCNTs were oxidized in 5 N HNO_3 solution for 3 h at room temperature and washed with boiling distilled water until the pH of the rinsed solution reached 6.0. These functionalized MWCNTs were dried in vacuum oven at 110 °C for 4 h.

Synthesis of FeSe/MWCNTs catalyst

20% FeSe/MWCNT's (Fe:Se = 1:1) catalyst was prepared by a procedure in which MPT and functionalized MWCNTs were dispersed in acetone by ultra-sonication. Temperature of the sonicator was kept at 80 °C. After complete evaporation of the solvent, the dried carbon powder was heat treated at 650 °C in argon

Table 2
Selected bond lengths (Å) and angles (°) for MPT.

Bond type	Distance (Å)	Bond type	Angle (°)
Se–C(17)	1.819(4)	H(1C)–N(1)–C(15)	117.0(3)
O–C(18)	1.219(4)	H(1C)–N(1)–C(17)	117.0(3)
N(1)–H1C	0.860(3)	Se–C(17)–N(2)	120.2(3)
N(2)–H2C	0.861(3)	Se–C(17)–N(1)	124.2(3)

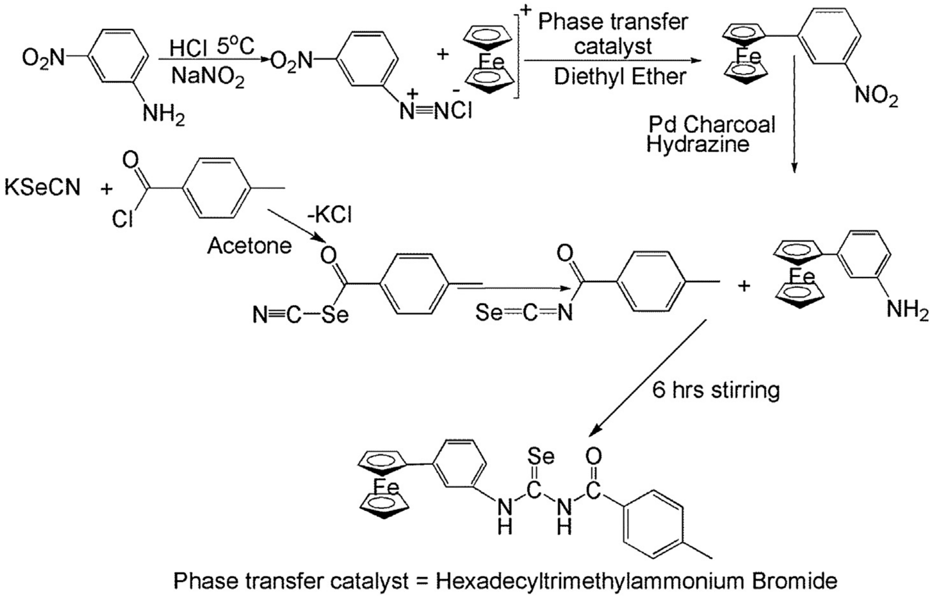

Scheme 1. Synthesis of 1-(4-methylbenzoyl)-3-(3-ferrocenylphenyl)selenourea.

atmosphere for 2 h [37]. This high temperature results in the decomposition of the complex and deposition of the iron and selenium in the form of iron selenide on the surface of MWCNTs.

Single cell testing

The synthesized 20% FeSe/MWCNTs catalyst was evaluated as cathode catalyst in H_2-O_2 fuel cell. 30% PtRu/MWCNTs was used as anode catalyst. 30% Pt/MWCNTs cathode catalysts was used for comparison. The metal loading on cathode was kept at 2 mg cm^{-2} while PtRu loading on anode side was also 2 mg cm^{-2}. Teflonized carbon paper (Toray) was used as electrode backing layer for anode and cathode. Catalyst ink was prepared by sonicating the catalyst in isopropanol and adding 10% nafion as binder. Catalyst ink was coated on the electrode by brush in multiple steps until the required loading was achieved. After drying the electrodes at 80 °C, nafion solution (5%) was applied to the electrode surface (3 mg cm^{-2}). Membrane electrode assembly was prepared by hot pressing the anode and cathode with nafion 115 membrane at 135 °C and 60 kg cm^{-2}. Single cell performance was evaluated in a laboratory made cell at 25 °C. Humidified hydrogen and oxygen were used as fuel and oxidant. Hydrogen and oxygen pressure was kept at 2 atm for anode and cathode respectively.

Photocatalytic degradation of MO

0.1 g of FeSe/MWCNTs catalyst was dispersed in 20 mL solution of MO in ethanol having absorbance value of ~1. This solution was placed under UV light of UVGL-58 254/365 nm at short wavelength mode under constant magnetic stirring in a dark room. The absorbance of this solution was measured after every 10 min on a UV-vis spectrophotometer.

Results and discussions

Characterization of MPT precursor

MPT was purified on the basis of its solubility (which is different from its precursors and byproducts) in common organic solvents. In ^{1}H NMR spectrum of MPT there are basically four different types of protons i.e. protons of −NH, ferrocene protons, aromatic protons and methyl protons. Maximum downfield proton is the proton of −NH (13.27 ppm) which is present between the C═O and C═Se groups whereas the other −NH appears slightly upfield (10.47 ppm) from it. Aromatic protons are available at their respective regions as multiplet and methyl group gives a singlet at 2.88 ppm. Unsubstituted cyclopentadienyl ring (Cp ring) of ferrocene yields a singlet whereas substituted Cp ring provides two triplets downfield from the singlet of unsubstituted Cp ring with a coupling constant of 1.8 Hz. In ^{13}C NMR maximum downfield carbon is the one which is attached with selenium (180.6) whereas carbonyl carbon appears 3–4 ppm upfield from it. Aromatic and methyl carbons are visible in their respective regions whereas unsubstituted Cp ring of ferrocene gives a singlet while substituted Cp provides three signals in which maximum downfield carbon is the one which is attached with the phenyl ring (84.3 ppm) [33–35].

In FTIR −NH protons provide a broad signal above 3200 cm^{-1} due to the presence of intermolecular and intramolecular hydrogen bonding. Aromatic protons yield a stretching band above 3000 cm^{-1} and aliphatic protons provide their signal at ~2900 cm^{-1}. Carbonyl carbon is available as an intense band at 1644 cm^{-1} whereas C═Se is available between 1000 and 1300 cm^{-1} [33–35]. Elemental concentrations, determined with CHNS analyzer and atomic absorption spectrophotometer, are in close agreement with calculated values.

XRD single crystal structure

Fig. 1 presents the ORTEP diagram of MPT which shows that protons of ferrocene moiety are not 100% eclipsed (protons are tilted at an angle of 0.33° only) and phenyl ring attached with Cp of ferrocene is tilted outside from the plane of Cp at an angle of 26.05°. Geometric arrangement of groups around C═Se is not symmetric i.e. the angle between the Se-C(17)-N(1) is 124.17° whereas the angle between the Se-C(17)-N(2) is 120.16°. There is an intramolecular hydrogen bond between the N(1) and O(1) which forms a six membered secondary ring. There are four molecules per unit cell of MPT which are arranged in a way that methyl of each molecule is emerging out of neighboring axial plane (Fig. 2a) whereas Fig. 2b represents the interactions in the stacked lattice.

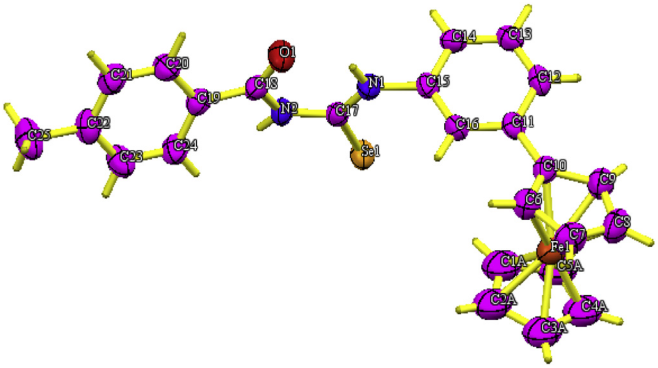

Fig. 1. Molecular diagram of MPT with ellipsoid displacement, non hydrogen atoms represented by 30% probability boundary spheres and hydrogen atoms are sticks of arbitrary size.

Characterization of FeSe supported on MWCNTs

Fig. 3a presents the PXRD of FeSe/MWCNTs which has prominent PbO type tetragonal phase. Minor peaks for hexagonal FeSe are also visible in the pattern [17]. The TGA pattern of MPT (Fig. 3b) provides a residual mass of 13.07% and if all the MPT is converted to FeSe then this residual mass should be 26.94%. This difference in the residual mass is due to the independent thermal evaporation of ferrocene moiety of MPT because when ferrocene molecule is subjected to the thermal treatment separately it vaporizes completely at 225 °C (red line (in the web version) in Fig. 3b). SEM image of FeSe/MWCNTs is given in Fig. 4a which shows uniform shape of the MWCNTs and homogeneous distribution of the FeSe NPs on them. TEM image presents the formation of FeSe NPs of less than 10 nm size on MWCNTs (Fig. 4b).

Applications of FeSe/MWCNTs

Fig. 5 shows a plot of absorbance vs. wavelength for photocatalytic degradation of MO. Figures of the beakers in the inset show the color of MO at time zero and after 80 min of treatment with FeSe/MWCNTs under UV light of 254 nm wavelength. It is evident from Fig. 5 that the degradation process is slower for first 20 min but after that it is comparatively very fast possibly due to higher concentration of the hydroxyl radicals formed after 20 min under UV light [9]. We observed that FeSe/MWCNTs catalyst is comparatively superior than the previously reported gold silver nano-core/silica nano-shell and same paper has given the mechanistic formation of methyl(phenyl)carbamic acid by the degradation of MO [9]. Self organized TiO_2 nanotubes (NTs) with Pd nanoparticles, Fe-doped TiO_2 NTs, Nd-doped TiO_2 NTs, La-doped TiO_2 NTs, Pt-doped TiO_2 NTs, Cu-doped TiO_2 NTs, ZnO/TiO_2 coupled oxides, Au-doped TiO_2 NTs, TiO_2/ZnO/Au nanofibers, Ag/AgCl/TiO_2 nanoparticles, Fe_3O_4/ZnO nanocomposites, different morphologies of ZnO (nanorod, nanodisc, porous octahedron) and Ag-doped ZnO have been previously reported for the degradation of MO [38,39]. But FeSe/MWCNTs catalyst is comparatively cheaper and easy to synthesize for industrial use in scrubbers and filters etc. to control the escape of azo compounds (dyes) into the environment.

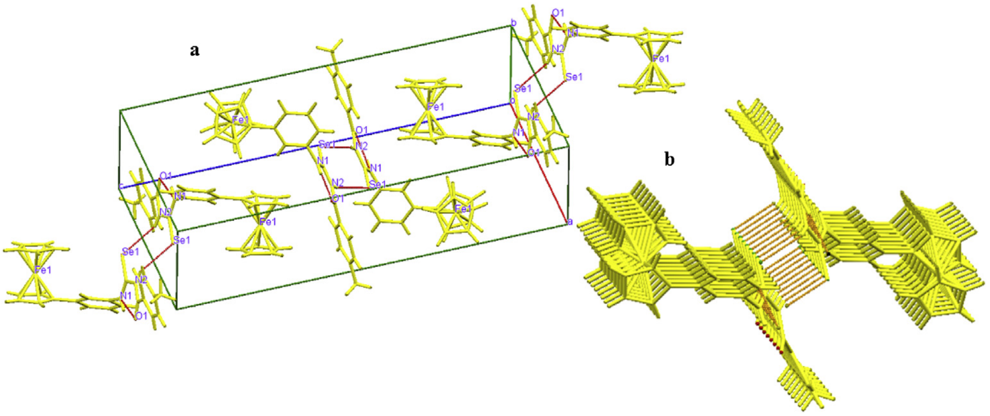

Fig. 2. a) Packing of MPT showing intermolecular interactions. b) Stacking in MPT.

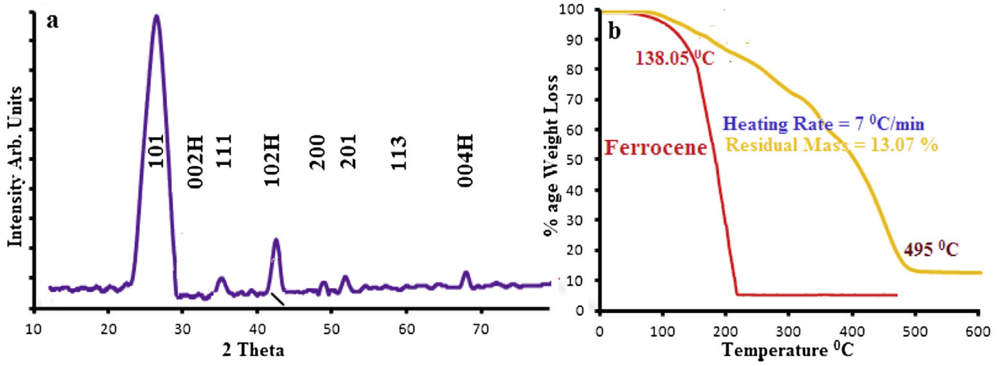

Fig. 3. a) Powder XRD of FeSe/MWCNTs, H stands for hexagonal phase of FeSe. b) Comparative TGA of MPT and ferrocene.

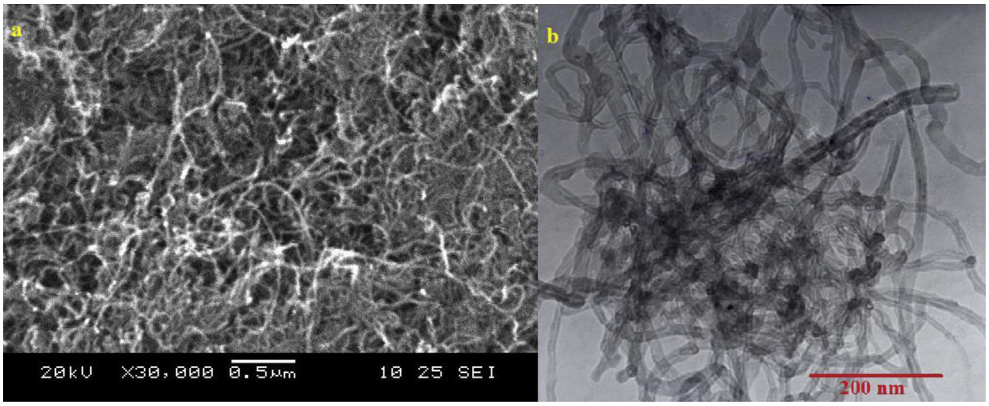

Fig. 4. a) SEM image of FeSe/MWCNTs. b) TEM image of FeSe/MWCNTs.

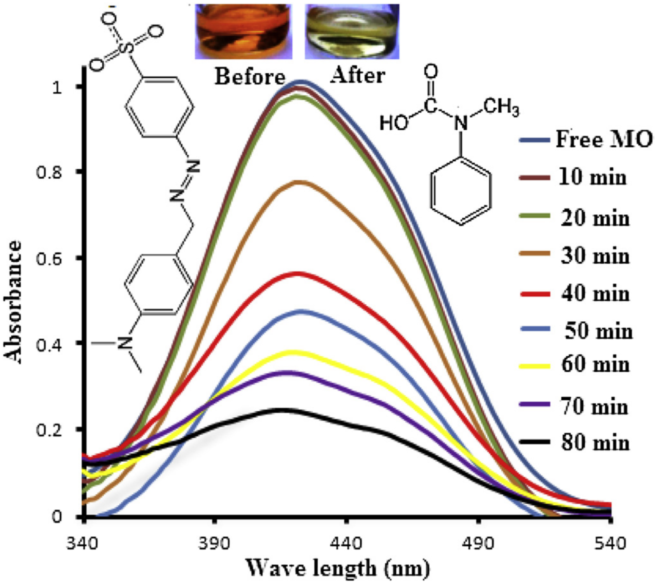

Fig. 5. Photocatalytic degradation of methyl orange by FeSe/MWCNTs with the help of UV-vis spectroscopy.

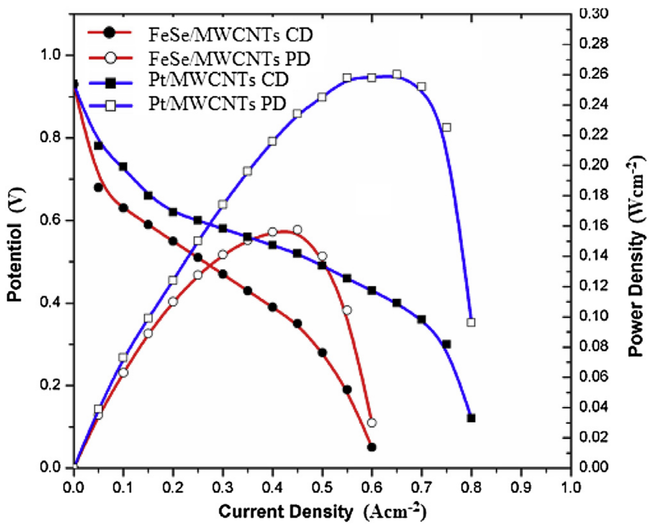

Fig. 6. Comparative polarization curves of FeSe/MWCNTs catalyst and Pt/MWCNTs catalysts.

Table 3
Comparative performance of the two catalysts.

Catalyst	Open circuit voltage	Current density (A cm^{-2})	Power density (W cm^{-2})
30% Pt/MWCNTs	0.975	0.8	0.250
20% FeSe/MWCNTs	0.952	0.6	0.157

Fig. 6 presents the comparative polarization curves of FeSe/MWCNTs and Pt/MWCNTs catalysts. The results have been summarized in Table 3 and show inferior performance of FeSe/MWCNTs in terms of power density, open circuit voltage and current density relative to Pt/MWCNTs catalyst, but Pt is too much costly as compared to Fe. We propose that the homogeneously alloyed blends of FeSe with Pt may improve the performance of FeSe/MWCNTs and reduce amount of Pt in the cathode and will ultimately reduce the cost [40–43].

Conclusions

We have successfully synthesized and characterized single source ferrocene incorporated selenourea precursor for the fabrication of FeSe/MWCNTs catalyst which has proved to be a good photocatalyst for the degradation of methyl orange and may replace the platinum metal from the electrodes of fuel cell in terms of its low cost. We have plans in the near future to synthesize the FeSe/Ni/Co/MWCNTs homogeneously alloyed materials to improve the performance of FeSe/MWCNTs.

References

[1] M. Winter, R.J. Brodd, Chem. Rev. 104 (2004) 4245–4270.
[2] W. Yu, M.D. Porosoff, J.G. Chen, Chem. Rev. 112 (2012) 5780–5817.
[3] L. Li, Y. Xing, J. Phys. Chem. C 111 (2007) 2803–2808.
[4] G. Buitrón, M. Quezada, G. Moreno, Bioresour. Technol. 92 (2004) 143–149.
[5] T. Sauer, G. Cesconeto Neto, H.J. José, R.F.P.M. Moreira, J. Photochem. Photobiol. A Chem. 149 (2002) 147–154.
[6] G. Tezcanli-Guyer, N.H. Ince, Ultrason. Sonochem. 10 (2003) 235–240.
[7] Y.M. Slokar, A. Majcen Le Marechal, Dyes Pigm. 37 (1998) 335–356.
[8] N. Kannan, M. Meenakshisundaram, Water Air Soil Pollut. 138 (2002) 289–305.
[9] Y. Badr, M.A. Mahmoud, J. Phys. Chem. Solids 68 (2007) 413–419.
[10] L. Chen, C.-F. Tsai, Y. Zhu, Z. Bi, H. Wang, Phys. C Supercond. 471 (2011) 515–519.
[11] T.-K. Chen, J.-Y. Luo, C.-T. Ke, H.-H. Chang, T.-W. Huang, K.-W. Yeh, C.-C. Chang, P.-C. Hsu, C.-T. Wu, M.-J. Wang, M.-K. Wu, Thin Solid Films 519 (2010) 1540–1545.
[12] P.Y. Chen, S.F. Hu, R.S. Liu, C.Y. Huang, Thin Solid Films 519 (2011) 8397–8400.
[13] S. Demura, H. Okazaki, T. Ozaki, H. Hara, Y. Kawasaki, K. Deguchi, T. Watanabe, S.J. Denholme, Y. Mizuguchi, T. Yamaguchi, H. Takeya, Y. Takano, Solid State Commun. 154 (2013) 40–42.

[14] X.J. Wu, Z.Z. Zhang, J.Y. Zhang, Z.G. Ju, B.H. Li, B.S. Li, C.X. Shan, D.X. Zhao, B. Yao, D.Z. Shen, Thin Solid Films 516 (2008) 6116–6119.

[15] Q.J. Feng, D.Z. Shen, J.Y. Zhang, C.X. Shan, Y.M. Lu, Y.C. Liu, X.W. Fan, J. Magn. Magn. Mater. 279 (2004) 435–439.

[16] X.J. Wu, Z.Z. Zhang, J.Y. Zhang, Z.G. Ju, D.Z. Shen, B.H. Li, C.X. Shan, Y.M. Lu, J. Cryst. Growth 300 (2007) 483–485.

[17] S.-M. Zhou, S.-Y. Lou, Y.-Q. Wang, X.-L. Chen, Mater. Lett. 65 (2011) 1741–1743.

[18] A.U. Ubale, Y.S. Sakhare, S.M. Bombatkar, Mater. Res. Bull. 48 (2013) 3564–3571.

[19] Y. Sakhare, A. Ubale, Arch. Phys. Res. 3 (2012) 452–458.

[20] N. Umeyama, M. Tomura, K. Takase, S. Hara, S. Horiguchi, A. Tominaga, H. Sato, Y. Hara, N. Miyakawa, S.I. Ikeda, Phys. C Supercond. 470 (Suppl. 1) (2010) S518–S520.

[21] A.U. Ubale, Y.S. Sakhare, J. Phys. Chem. Solids 74 (2013) 1459–1464.

[22] Z. Li, J. Ju, J. Tang, K. Sato, M. Watahiki, K. Tanigaki, J. Phys. Chem. Solids 71 (2010) 495–498.

[23] S. Agatsuma, T. Yamagishi, S. Takeda, M. Naito, Phys. C Supercond. 470 (2010) 1468–1472.

[24] X. Qi, J.-Y. Wang, J.-C. Kuo, K.A. Yates, L.F. Cohen, J. Alloys Compd. 509 (2011) 6350–6353.

[25] C.-C. Chang, C.-H. Wang, M.-H. Wen, Y.-R. Wu, Y.-T. Hsieh, M.-K. Wu, Solid State Commun. 152 (2012) 649–652.

[26] R. Yoshida, T. Wakita, H. Okazaki, Y. Mizuguchi, S. Tsuda, Y. Takano, H. Takeya, K. Hirata, Y. Kato, T. Muro, M. Okawa, K. Ishizaka, S. Shin, H. Harima, M. Hirai, Y. Muraoka, T. Yokoya, Phys. C Supercond. 470 (Suppl. 1) (2010) S389–S390.

[27] Q. Dong, G. Li, C.-L. Ho, M. Faisal, C.-W. Leung, P.W.-T. Pong, K. Liu, B.-Z. Tang, I. Manners, W.-Y. Wong, Adv. Mater. 24 (2012) 1034–1040.

[28] K. Liu, C.-L. Ho, S. Aouba, Y.-Q. Zhao, Z.-H. Lu, S. Petrov, N. Coombs, P. Dube, H.E. Ruda, W.-Y. Wong, I. Manners, Angew. Chem. Int. Ed. 47 (2008) 1255–1259.

[29] A.N. Gleizes, Chem. Vap. Depos. 6 (2000) 155–173.

[30] Siemens Analytical X-ray Instruments, Inc, Analytical Chemistry, vol. 61, 1989, p. 1309A.

[31] A.A. Altaf, A. Badshah, N. Khan, M.N. Tahir, Acta Crystallogr. Sect. E Struct. Rep. Online 66 (2010) m831.

[32] B. Lal, A. Badshah, A.A. Altaf, M.N. Tahir, S. Ullah, F. Huq, Dalton Trans. 41 (2012) 14643–14650.

[33] R.A. Hussain, A. Badshah, M. Sohail, B. Lal, K. Akbar, J. Mol. Struct. 1048 (2013) 367–374.

[34] R.A. Hussain, A. Badshah, M.N. Tahir, B. Lal, I.A. Khan, Aust. J. Chem. 66 (2013) 626–634.

[35] R.A. Hussain, A. Badshash, M. Sohail, B. Lal, A.A. Altaf, Inorg. Chim. Acta 402 (2013) 133–139.

[36] R.A. Hussain, A. Badshah, M.N. Tahir, T.U Hassan, A. Bano, J. Biochem. Mol. Toxicol. 28 (2014) 60–68.

[37] Q. Dong, G. Li, C.-L. Ho, C.-W. Leung, P.W.-T. Pong, I. Manners, W.-Y. Wong, Adv. Funct. Mater. 24 (2014) 857–862.

[38] C.W. Lai, J.C. Juan, W.B. Ko, S. Bee Abd Hamid, Int. J. Photoenergy 2014 (2014).

[39] S. Singh, K. Barick, D. Bahadur, J. Mater. Chem. A 1 (2013) 3325–3333.

[40] V. Kamavaram, V. Veedu, A.M. Kannan, J. Power Sources 188 (2009) 51–56.

[41] J.F. Lin, V. Kamavaram, A.M. Kannan, J. Power Sources 195 (2010) 466–470.

[42] B.R. Matos, E.I. Santiago, J.F.Q. Rey, A.S. Ferlauto, E. Traversa, M. Linardi, F.C. Fonseca, J. Power Sources 196 (2011) 1061–1068.

[43] M.S. Saha, R. Li, X. Sun, J. Power Sources 177 (2008) 314–322.